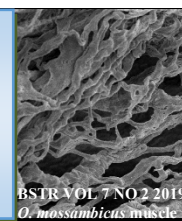


BIOREMEDIATION SCIENCE AND TECHNOLOGY RESEARCH

Website: <https://journal.hibiscuspublisher.com/index.php/BSTR>



Modelling the Growth Inhibition Kinetics of *Rhodotorula* sp. strain MBH23 (KCTC 11960BP) on Acrylamide

Othman, A.R.^{1*} and Rahim, M.B.H.A.²

¹Department of Chemical Engineering and Process, Faculty of Engineering and Built Environment, Universiti Kebangsaan Malaysia, 43600 UKM Bangi, Selangor, D.E, Malaysia.

²Department of Biochemistry, Faculty of Biotechnology and Biomolecular Sciences, Universiti Putra Malaysia, UPM 43400 Serdang, Selangor, Malaysia.

*Corresponding author:

Dr. Ahmad Razi Othman

Department of Chemical Engineering and Process,
Faculty of Engineering and Built Environment,
Universiti Kebangsaan Malaysia,
43600 UKM Bangi, Selangor, D.E,
Malaysia.

Email: ahmadrazi@ukm.edu.my

HISTORY

Received: 24th August 2019
Received in revised form: 7th of October 2019
Accepted: 5th of December 2019

KEYWORDS

Rhodotorula sp.
Acrylamide-degrading
modified Gompertz
Haldane
modelling

ABSTRACT

The yeast *Rhodotorula* sp. Strain MBH23 (KCTC 11960BP) is an efficient acrylamide-degrader and is able to tolerate high concentrations of acrylamide. A primary modelling exercise for the growth of this yeast on acrylamide yields important specific growth rates which were utilized successfully for secondary modelling exercise which gave Luong as the best model. The Luong's constants; maximal growth rate, half-saturation constant for maximal growth, maximal concentration of substrate tolerated and curve parameter that defines the steepness of the growth rate decline from the maximum rate symbolized by μ_{max} , K_s , S_m , and n (\pm standard error) were $0.099 \pm 0.017 \text{ hr}^{-1}$, $17.34 \pm 5.0 \text{ mg/L}$, $2053.0 \pm 56.0 \text{ mg/L}$ and 0.801 ± 0.202 , respectively. The Luong model indicates that acrylamide is toxic and inhibits the growth of this yeast. To date, this is the first time that such a modelling exercise was utilized to model growth kinetics on acrylamide.

INTRODUCTION

Concern towards environmental problems is continuously growing due to the release of thousands of different toxic compounds as a result of human activities every day. Demands on the sustainable and controllable solutions to combat the environmental pollution which have minimal effect on the environment are highly sought after. Biodegradation is defined as a process of the disintegration of materials by the microorganism or other biological actions [1]. It is one of the established approaches for removal of undesirable organic compounds to the level that it can no longer be detected or within the maximum allowable limit set by the regulatory agencies [2].

Acrylamide ($\text{CH}_2=\text{CHCONH}_2$) is an amide group consisting of three-carbon compound with an α , β -unsaturated olefin bond. This compound is used as a commercial conjugated reactive molecule for the production of polymers especially polyacrylamide [3–5]. In industry, acrylamide has been used worldwide as a binding, thickening, and flocculating agent [6,7]. Acrylamide is also utilized in wastewater treatment method, pesticide ingredients, cosmetic makeup products, sugar production, and also to protect against soil deterioration. The

prevalent utilization of acrylamide and its polymer (polyacrylamide) has resulted in the pollution of terrestrial and aquatic surroundings [3,4]. Acrylamide is a rising harmful pollutant. This poisonous substance could get into the body of a human by means of absorption by means of skin, lungs, and the digestive tract [8]. The exposure of human to acrylamide takes place mostly in place of work coming from skin touching the acrylamide monomer and from breathing in dust as well as vapor. Acrylamide is a known neurotoxicant, carcinogen and teratogen in mammals [6].

Acrylamide exerts its toxic effect when it is oxidized to the epoxide glycidamide that catalyzed by an enzymatic reaction involving cytochrome P450 2E1 [9]. Previous studies showed that acrylamide and its oxidized form glycidamide caused abnormalities in the daughter cells of animals and plants [10]. In view of the fact that acrylamide is toxic to human health, this compound needs to be removed from the environment. Previously, several microorganisms such as *Pseudomonas* sp. [11], *Pseudomonas stutzeri* [12], *Pseudonocardia thermophila* [13], *Bacillus cereus* [14], and the fungi *Aspergillus oryzae* [15], which are capable of utilizing acrylamide a source of carbon and/or nitrogen have successfully been isolated. Moreover, our

group has also been successfully isolated and characterized an acrylamide-degrading yeast *Rhodotorula* sp. Strain MBH23 (KCTC 11960BP) [16].

Recently, a number of mathematical models have been utilized in order to explain the metabolism of compounds exposed to microbial populations in the natural environment. One of the most widely used mathematical equation in describing substrate utilization linked to growth rate is the Monod equation [17]. However, the limitation of this method is that it cannot be used for biodegradation process that shows substrate inhibition towards the rate. Due to this limitation, a model such as the Haldane or other substrate-inhibiting models such as Aiba, Webb (Edward), Teissier Yano and Koga, Hans-Levenspiel and Luong have been preferably used [18,19]. Hence, the utilization of considerable models available could replace the Haldane in some circumstances and discloses mechanistic process. In the present study, the growth of strain MBH23 (KCTC 11960BP) was inhibited when the acrylamide concentration in the growth media was increased to 2000 mg/L.

The inhibition of the bacterial growth rate caused by the high phenol concentration has not been seen in many phenol biodegradation studies using *Pseudomonas* sp. bacteria model, where the Haldane and other kinetics model have been used instead of models that allow for the complete abolishment of growth rates such as Luong, Teissier and Han-Levenspiel. This is probably due to the well-perceived notion that the *Pseudomonas* genus is highly tolerant to toxicants including phenol [20–34]. In order to obtain more accurate data, the bacteria growth rates on phenol were determined by employing the modified Gompertz model as a nonlinear curve fitting model [28,35–42]. In many previous phenol biodegradation studies, the growth rates were obtained by taking the linear portion of the natural logarithm of cellular biomass, which is done manually. Using the growth rates data, several available growth kinetic models were then evaluated. To date, limited statistical tests were used to accept the best model in modelling the kinetics of phenol biodegradation, and the most commonly used test is the coefficient of determination (R^2) [43,44].

However, by using this coefficient of determination (R^2), the number of parameters used in the model needs to be adjusted [45–47]. This adjustment can be made using an adjusted coefficient of determination ($\text{adj}R^2$), root mean square error RMSE, Corrected Akaike Information Criteria (AICc) and others. Based on the data obtained in this study, Luong model was found to be the best model to study the phenol biodegradation by the bacteria. In addition, the use of nonlinear regression fitting and assessment of the best model based on statistical tests relies heavily on the premise that the residuals are normally distributed. Thus, three commonly used statistical diagnosis tests for normality which are Wilks-Shapiro, Kolmogorov-Smirnov, and D'Agostino-Pearson were performed on the residuals from the Luong model. This present study suggests that in order to obtain an accurate and more reliable data, future selection of the best kinetic model governing the growth rates on toxicants especially acrylamide should be done comprehensively.

MATERIALS AND METHODS

Growth and maintenance of acrylamide-degrading yeast

The yeast *Rhodotorula* sp. Strain MBH23 (KCTC 11960BP) was maintained in minimal salts medium (MSM). The MSM (pH 7.5) with glucose autoclaved separately is composed of (per liter): 6.8 g of KH_2PO_4 (BDH), 10 g of glucose (BDH (British Drug House),

Poole, UK), 0.005 g of $\text{FeSO}_4 \cdot \text{H}_2\text{O}$ (BDH), 0.5 g of $\text{MgSO}_4 \cdot 7\text{H}_2\text{O}$ (BDH), 0.5 g acrylamide as the sole nitrogen source with 1 mL of the following trace elements (per liter): 0.003 g of $\text{CoCl}_2 \cdot 6\text{H}_2\text{O}$, 0.01 g of $\text{Cu}(\text{CH}_3\text{COO})_2 \cdot \text{H}_2\text{O}$ 0.03 g of ZnCl_2 (BDH); 0.002 g of $\text{FeCl}_2 \cdot 6\text{H}_2\text{O}$ (JT Baker) and 0.05 g of H_3BO_3 (JT Baker, John Townsend Baker, Phillipsburg, N.J., U.S.A.) [48]. In order to avoid degradation via heating, acrylamide was sterilized by passing through a 0.45 μm polytetrafluoroethylene (PTFE) syringe filter. The culture was incubated on a shaking incubator (Certomat R, USA) at room temperature (28 °C) at 150 rpm for 72 h [16].

Growth kinetics on acrylamide

The yeast growth kinetics on acrylamide was studied using a batch culture of the yeast supplemented with acrylamide at concentrations up to 1000 mg/L. The modified Gompertz model was utilised in the secondary inhibition kinetics modelling to obtain the growth parameter maximum specific growth rate or μ_m . The equation is as follows;

$$y = A \exp \left\{ - \exp \left[\frac{\mu_m e}{A} (\lambda - t) + 1 \right] \right\} \quad (1)$$

The values obtained from this primary modelling exercise was then used to model various growth kinetics model as follows;

Table 1. Kinetic models for growth of yeast on acrylamide.

Author	Degradation Rate	Ref
Monod	$\mu_{\max} \frac{S}{K_s + S}$	[17]
Haldane	$\mu_{\max} \frac{S}{S + K_s + \frac{S^2}{K_i}}$	[49]
Teissier	$\mu_{\max} \left(1 - \exp \left(- \frac{S}{K_i} \right) - \exp \left(- \frac{S}{K_s} \right) \right)$	[50,51]
Aiba	$\mu_{\max} \frac{S}{K_s + S} \exp(-KP)$	[52]
Yano and Koga	$\frac{\mu_{\max} S}{S + K_s + \left(\frac{S^2}{K_1} \right) \left(1 + \frac{S}{K} \right)}$	[53]
Luong	$\mu_{\max} \frac{S}{S + K_s} \left[1 - \left(\frac{S}{S_m} \right)^n \right]$	[54]

Note:
 μ_{\max} maximal growth rate (h^{-1})
 K_s half saturation constant for maximal degradation (mg/L)
 S_m maximal concentration of substrate tolerated and (mg/L)
 m, n, K curve parameters
 S substrate concentration (mg/L)
 P product concentration (mg/L)

Fitting of the data

Nonlinear regression was carried out using the CurveExpert Professional software (Version 1.6), which utilizes the Marquardt algorithm to fit the Gompertz and several inhibition kinetics models (Table 1) by nonlinear regression. This algorithm reduces the sums of squares of the residuals.

Statistics of the growth kinetics

Statistical analysis of the growth models' residuals was carried out to select the best model, using approaches such as the corrected Akaike Information Criterion or AICc, adjusted coefficient of determination (R^2), root-mean-square error (RMSE) accuracy factor (AF) and bias factor (BF). Statistical diagnosis tests for normality which are Wilks-Shapiro, Kolmogorov-Smirnov, and D'Agostino-Pearson were performed on the residuals from the Luong model [55].

The RMSE was calculated according to equation 2,

$$RMSE = \sqrt{\frac{\sum_{i=1}^n (Pd_i - Ob_i)^2}{n - p}} \tag{2}$$

where

- n number of experimental data
- Pd_i predicted values by the model
- Ob_i experimental data
- p parameters number of the model

In general, the model having the smaller number of parameter results in a smaller RMSE value [56].

The coefficient of determination or R^2 although popular the method does not consider the number of parameters of models in nonlinear regression, and therefore does not readily offer comparative evaluation. To get over this problem, an adjusted R^2 which takes into consideration the quantity of parameter of models is utilized to calculate the quality of nonlinear models based on the formula below;

$$Adjusted (R^2) = 1 - \frac{RMS}{s_y^2} \tag{3}$$

$$Adjusted (R^2) = 1 - \frac{(1 - R^2)(n - 1)}{(n - p - 1)} \tag{4}$$

where

S_y^2 is the total variance of the y-variable and RMS is the Residual Mean Square

The Akaike information criterion (AIC) is established upon information theory. The formula incorporates some variables penalty where the more the variables, the higher the AIC value. In studies where the data is small a corrected version of AIC; the Akaike information requirements (AIC) with correction or AICc is utilised instead [57]. AICc is calculated using the following equation;

$$AICc = 2p + n \ln \left(\frac{RSS}{n} \right) + 2(p+1) + \frac{2(p+1)(p+2)}{n-p-2} \tag{5}$$

Where

- n number of data points
- p parameter numbers of the model

The Accuracy Factor (AF) and Bias Factor (BF) are another goodness-of-fit exercises for models (Ross and McMeekin, 1994). The statistics calculates the perfect match between experimental and predicted values. As a rule, a BF value > 1.0 indicates a model which is fail-safe a value < 1.0 indicates a model that is fail-dangerous. On the other hand, the AF is always ≥ 1.0 , with precise models giving values nearing to 1.0.

$$Bias\ factor = 10^{\left(\sum_{i=1}^n \log \frac{(Pd_i / Ob_i)}{n} \right)} \tag{6}$$

$$Accuracy\ factor = 10^{\left(\sum_{i=1}^n \log \frac{|(Pd_i / Ob_i)|}{n} \right)} \tag{7}$$

RESULTS AND DISCUSSION

Growth kinetics

The specific growth rate was obtained from a primary modelling exercise using the modified Gompertz model (Fig. 1) as this model has often been used to model growth curve on xenobiotics as a substrate [58,59].

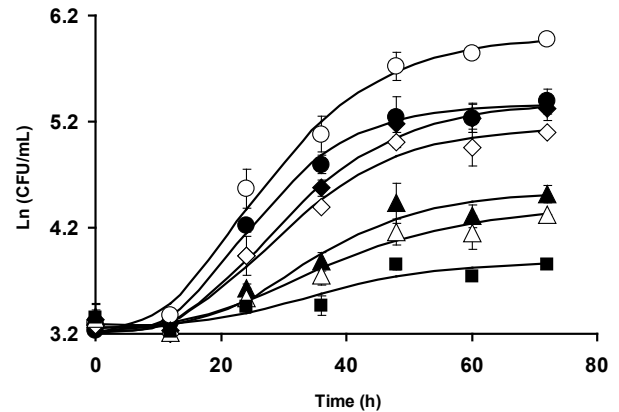


Fig. 1. Growth of *Rhodotorula* sp. Strain MBH23 on various acrylamide concentrations (200 (●), 300 (○), 400 (◆), 500 (◇), 600 (▲), 700 (△) and 800 (■) mg/L) modelled according to the modified Gompertz model (line). Error bars indicate mean standard deviation (n=3).

The primary modelling exercise yields important specific growth rates which were then plotted against the initial acrylamide concentrations. A secondary modelling exercise utilizing various kinetics models was then carried out (Figs. 2-7). The statistical analysis and accuracy of the all six kinetic models used indicated that Luong was the best model with small values for RMSE and AICc, uppermost adjusted R^2 values, F-test and with Bias Factor and Accuracy Factor nearest to unity (1.0) (Table 2).

The Luong's constants; maximal growth rate, half-saturation constant for maximal growth, maximal concentration of substrate tolerated and curve parameter that defines the steepness of the growth rate decline from the maximum rate symbolized by μ_{max} , K_s , S_m , and n (\pm standard error) were $0.099 \pm 0.017 \text{ hr}^{-1}$, $17.34 \pm 5.0 \text{ mg/L}$, $2053.0 \pm 56.0 \text{ mg/L}$ and 0.801 ± 0.202 , respectively. Models such as Luong, Teissier and Hans-Levenspiel were developed due to the limitations of previous models such Haldane, Andrews and Noack, Web, and Yano in that these models failed to explain some situations where growth rate became zero at very high substrate concentration

[60]. To date, this is the first time that such a modelling exercise was utilized to model growth kinetics on acrylamide. Modelling of bacterial growth kinetics on xenobiotics is an important aspect of designing effective bioremediation strategy as the constants obtained can be utilized to plan and understand the limitations of bioremediation [19].

Table 2. Statistical analysis of kinetic models.

Model	<i>p</i>	RMSE	<i>R</i> ²	<i>adR</i> ²	AF	BF	AICc
Luong	4	0.011	1.00	0.99	-59.11	1.00	1.03
Aiba	3	0.013	0.96	0.94	-47.19	0.98	1.04
Haldane	3	0.011	0.97	0.96	45.45	1.00	1.15
Han and Levenspiel	4	0.025	0.87	0.75	-33.12	1.00	1.15
Yano	4	0.025	0.87	0.75	-35.16	1.00	1.15
Teissier	4	0.025	0.89	0.79	-33.44	0.89	1.22
Monod	2	0.063	-4.09	-5.78	-36.17	0.89	1.54

Note:
 SSE Sums of Squared Errors
 RMSE Root Mean Squared Error
*R*² Coefficient of Determination
*adR*² Adjusted Coefficient of Determination
 AICC Corrected Akaike Information Criterion
 BF Bias Factor
 AF Accuracy Factor

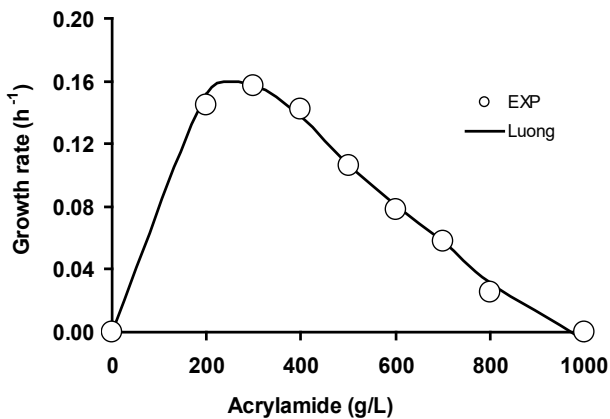


Fig. 3. Curve fitting of the growth rate of *Rhodotorula* sp. Strain MBH23 on acrylamide using the Luongs's model.

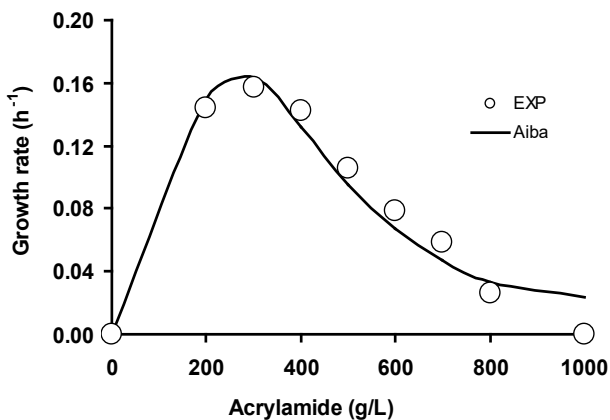


Fig. 2. Curve fitting of the growth rate of *Rhodotorula* sp. Strain MBH23 on acrylamide using the Aiba's model.

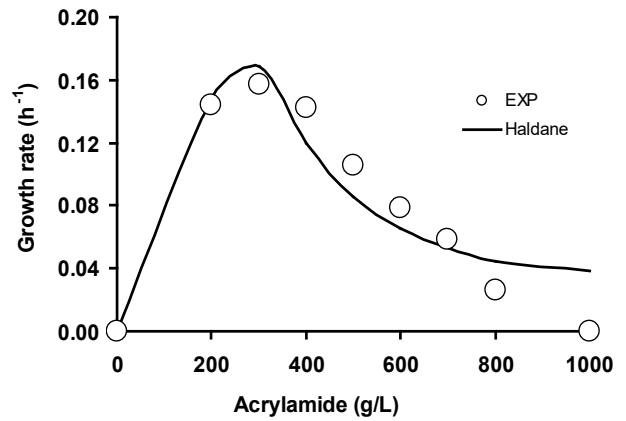


Fig. 3. Curve fitting of the growth rate of *Rhodotorula* sp. Strain MBH23 on acrylamide using the Haldane's model.

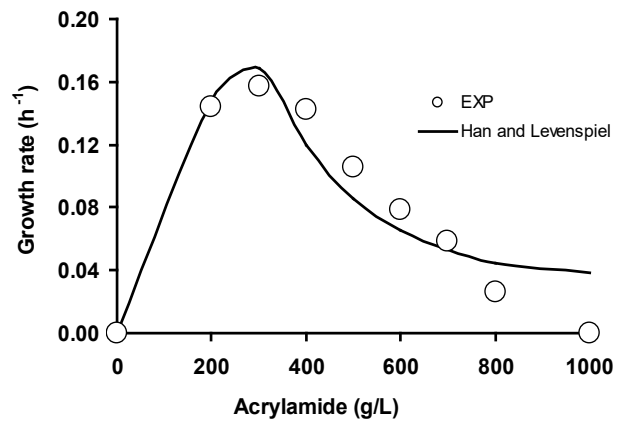


Fig. 4. Curve fitting of the growth rate of *Rhodotorula* sp. Strain MBH23 on acrylamide using the Hans and Levenspiel's model.

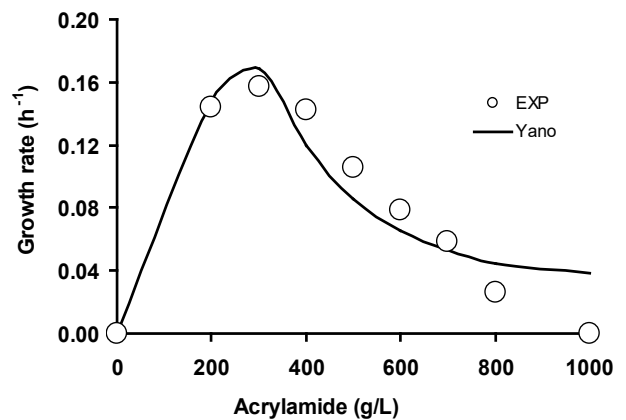


Fig. 5. Curve fitting of the growth rate of *Rhodotorula* sp. Strain MBH23 on acrylamide using the Yano's model.

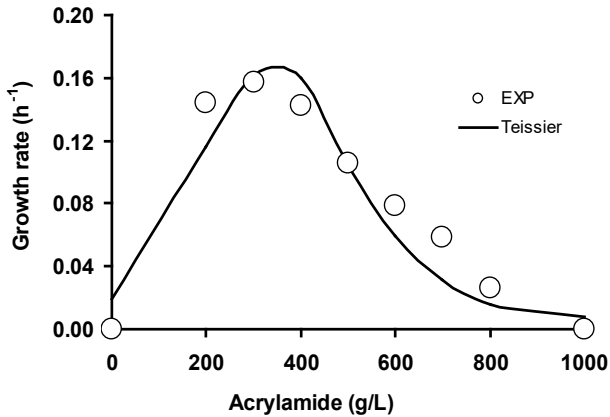


Fig. 6. Curve fitting of the growth rate of *Rhodotorula* sp. Strain MBH23 on acrylamide using the Teissier's model.

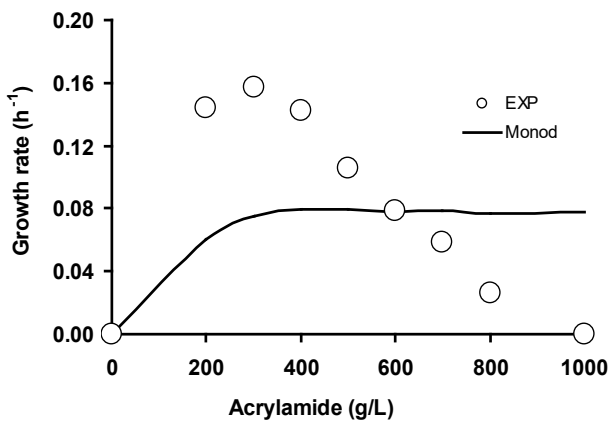


Fig. 7. Curve fitting of the growth rate of *Rhodotorula* sp. Strain MBH23 on acrylamide using the Monod's model.

CONCLUSION

In conclusion, the primary modelling exercise for the growth of this yeast on acrylamide yields important specific growth rates which were utilized successfully for secondary modelling exercise which gave Luong as the best model. The Luong's constants; maximal growth rate, half-saturation constant for maximal growth, maximal concentration of substrate tolerated and curve parameter that defines the steepness of the growth rate decline from the maximum rate symbolized by μ_{max} , K_s , S_m , and n (\pm standard error) were $0.099 \pm 0.017 \text{ hr}^{-1}$, $17.34 \pm 5.0 \text{ mg/L}$, $2053.0 \pm 56.0 \text{ mg/L}$ and 0.801 ± 0.202 , respectively. The Luong model indicates that acrylamide is toxic and inhibits the growth of this yeast. To date, this is the first time that such a modelling exercise was utilized to model growth kinetics on acrylamide.

REFERENCES

1. Vert M, Doi Y, Hellwich K-H, Hess M, Hodge P, Kubisa P, et al. Terminology for biorelated polymers and applications (IUPAC Recommendations 2012). *Pure Appl Chem*. 2012; 84(2):377-410
2. Buranasilp K, Charoenpanich J. Biodegradation of acrylamide by *Enterobacter aerogenes* isolated from wastewater in Thailand. *J Environ Sci*. 2011;23(3):396-403.
3. Igisu H, Matsuoka M. Acrylamide Encephalopathy. *Sangyo Eiseigaku Zasshi*. 2002;44(2):A21.
4. Kotlova EK, Chestukhina GG, Astaurova OB, Leonova TE, Yanenko AS, Debabov VG. Isolation and primary characterization of an amidase from *Rhodococcus rhodochrous*. *Biochem Biokhimiia*. 1999 Apr;64(4):384-9.

5. Weideborg M, Källqvist T, Ødegård KE, Sverdrup LE, Vik EA. Environmental risk assessment of acrylamide and methylolacrylamide from a grouting agent used in the tunnel construction of romeriksporten, norway. *Water Res*. 2001 Aug;35(11):2645-52.
6. Sathesh Prabu C, Thatheyus AJ. Biodegradation of acrylamide employing free and immobilized cells of *Pseudomonas aeruginosa*. *Int Biodeterior Biodegrad*. 2007 Jan;60(2):69-73.
7. Wampler DA, Ensign SA. Photoheterotrophic Metabolism of Acrylamide by a Newly Isolated Strain of *Rhodopseudomonas palustris*. *Appl Environ Microbiol*. 2005 Oct 1;71(10):5850-7.
8. Charoenpanich J. Removal of Acrylamide by Microorganisms. In: Patil Y, editor. *Applied Bioremediation - Active and Passive Approaches* [Internet]. InTech; 2013 [cited 2017 Dec 18]. Available from: <http://www.intechopen.com/books/applied-bioremediation-active-and-passive-approaches/removal-of-acrylamide-by-microorganisms>
9. Besaratinia A, Pfeifer GP. Genotoxicity of acrylamide and glycidamide. *J Natl Cancer Inst*. 2004 Jul 7;96(13):1023-9.
10. Bergmark E, Calleman CJ, Costa LG. Formation of hemoglobin adducts of acrylamide and its epoxide metabolite glycidamide in the rat. *Toxicol Appl Pharmacol*. 1991 Nov;111(2):352-63.
11. Shukor MY, Gusmanizar N, Ramli J, Shamaan NA, MacCormack WP, Syed MA. Isolation and characterization of an acrylamide-degrading Antarctic bacterium. *J Environ Biol*. 2009 Jan;30(1):107-12.
12. Wang CC, Lee CM. Denitrification with acrylamide by pure culture of bacteria isolated from acrylonitrile-butadiene-styrene resin manufactured wastewater treatment system. *Chemosphere*. 2001 Aug;44(5):1047-53.
13. Egorova K, Trauthwein H, Verseck S, Antranikian G. Purification and properties of an enantioselective and thermoactive amidase from the thermophilic actinomycete *Pseudonocardia thermophila*. *Appl Microbiol Biotechnol*. 2004 Jul;65(1):38-45.
14. Shukor MY, Gusmanizar N, Azmi NA, Hamid M, Ramli J, Shamaan NA, et al. Isolation and characterization of an acrylamide-degrading *Bacillus cereus*. *J Environ Biol*. 2009 Jan;30(1):57-64.
15. Wakaizumi M, Yamamoto H, Fujimoto N, Ozeki K. Acrylamide degradation by filamentous fungi used in food and beverage industries. *J Biosci Bioeng*. 2009 Nov;108(5):391-3.
16. Rahim MBH, Syed MA, Shukor MY. Isolation and characterization of an acrylamide-degrading yeast *Rhodotorula* sp. strain MBH23 KCTC 11960BP. *J Basic Microbiol*. 2012;52(5):573-81.
17. Monod J. The Growth of Bacterial Cultures. *Annu Rev Microbiol*. 1949;3(1):371-94.
18. Gunasekaran B, Shukor MS, Masdor NA, Shamaan NA, Shukor MY. Test of randomness of residuals for the Buchanan-three-phase model used in the fitting the growth of *Paracoccus* sp. SKG on acetonitrile. *J Environ Bioremediation Toxicol*. 2015;3(1):12-14.
19. Halmi MIE, Shukor MS, Masdor NA, Shamaan NA, Shukor MY. Evaluation of several mathematical models for fitting the growth of sludge microbes on PEG 600. *J Environ Microbiol Toxicol*. 2015;3(1):1-5.
20. Agarry SE, Audu TOK, Solomon BO. Substrate inhibition kinetics of phenol degradation by *Pseudomonas fluorescence* from steady state and wash-out data. *Int J Environ Sci Technol*. 2009;6(3):443-50.
21. Gafar AA, Manogaran M, Yasid NA, Halmi MIE, Shukor MY, Othman AR. Arrhenius plot analysis, temperature coefficient and Q10 value estimation for the effect of temperature on the growth rate on acrylamide by the Antarctic bacterium *Pseudomonas* sp. strain DRYJ7. *J Environ Microbiol Toxicol*. 2019 Jul 31;7(1):27-31.
22. Kesavan V, Mansur A, Suhaili Z, Salihan MSR, Rahman MFA, Shukor MY. Isolation and Characterization of a Heavy Metal-reducing *Pseudomonas* sp. strain Dr.Y Kertih with the Ability to Assimilate Phenol and Diesel. *Bioremediation Sci Technol Res*. 2018 Jul 31;6(1):14-22.
23. Yasid NA, Ahmad SA, Saruni NH, Abd Razak NS, Shukor MY. Comparison of biosurfactants produced by the Antarctic hydrocarbon-degrading *Pseudomonas* sp. ADL15 and *Rhodococcus* sp. ADL36 and their characterization. In 10-3 Midori-cho, Tachikawa, Tokyo, Japan: National Institute of Polar Research (NIPR); 2018. Available from: <http://id.nii.ac.jp/1291/00015257/>

24. Içgen B, Salik SB, Goksu L, Ulusoy H, Yilmaz F. Higher alkyl sulfatase activity required by microbial inhabitants to remove anionic surfactants in the contaminated surface waters. *Water Sci Technol J Int Assoc Water Pollut Res.* 2017 Nov;76(9–10):2357–66.
25. Zhang C, Wang B, Dai X, Li S, Lu G, Zhou Y. Structure and function of the bacterial communities during rhizoremediation of hexachlorobenzene in constructed wetlands. *Environ Sci Pollut Res.* 2017 Apr 1;24(12):11483–92.
26. Yakasai MH, Rahman MFA, Rahim MBHA, Khayat ME, Shamaan NA, Shukor MY. Isolation and characterization of a metal-reducing *Pseudomonas* sp. strain 135 with amide-degrading capability. *Bioremediation Sci Technol Res.* 2017;5(2):32–38.
27. Jiang B, Li A, Cui D, Cai R, Ma F, Wang Y. Biodegradation and metabolic pathway of sulfamethoxazole by *Pseudomonas psychrophila* HA-4, a newly isolated cold-adapted sulfamethoxazole-degrading bacterium. *Appl Microbiol Biotechnol.* 2014;98(10):4671–81.
28. Calvayrac C, Romdhane S, Barthelmebs L, Rocaboy E, Cooper J-F, Bertrand C. Growth abilities and phenotype stability of a sulcotriene-degrading *Pseudomonas* sp. isolated from soil. *Int Biodeterior Biodegrad.* 2014;91:104–10.
29. Liu J, Wang Q, Yan J, Qin X, Li L, Xu W, et al. Isolation and characterization of a novel phenol degrading bacterial strain WUST-C1. *Ind Eng Chem Res.* 2013;52(1):258–65.
30. Hussain S, Maqbool Z, Ali S, Yasmeen T, Imran M, Mahmood F, et al. Biodecolorization of reactive black-5 by a metal and salt tolerant bacterial strain *Pseudomonas* sp. RA20 isolated from Paharang drain effluents in Pakistan. *Ecotoxicol Environ Saf.* 2013;98:331–8.
31. Leena R, Raj DS. Biological decolourisation of two synthetic textile dyes and an actual textile dyeing industry effluent by selected bacterial isolates. *Nat Environ Pollut Technol.* 2009;8(3):399–406.
32. Kotresha D, Vidyasagar GM. Isolation and characterisation of phenol-degrading *Pseudomonas aeruginosa* MTCC 4996. *World J Microbiol Biotechnol.* 2008;24(4):541–7.
33. Yang C-F, Lee C-M. Enrichment, isolation, and characterization of phenol-degrading *Pseudomonas resinovorans* strain P-1 and *Brevibacillus* sp. strain P-6. *Int Biodeterior Biodegrad.* 2007;59(3 SPEC. ISS.):206–10.
34. Kolić NU, Hršak D, Kolar AB, Petrić I, Stipičević S, Soulas G, et al. Combined metabolic activity within an atrazine-mineralizing community enriched from agrochemical factory soil. *Int Biodeterior Biodegrad.* 2007;60(4):299–307.
35. Zhu H, Yang J, Xiaowei C. Application of Modified Gompertz Model to Study on Biogas production from middle temperature co-digestion of pig manure and dead pigs. 2019. In *E3S Web of Conferences* (Vol. 118, p. 03022). EDP Sciences.
36. Shukor MY. Bartlett and the Levene's tests of homoscedasticity of the modified Gompertz model used in fitting of *Burkholderia* sp. strain Neni-11 growth on acrylamide. *Bioremediation Sci Technol Res.* 2016 Jul 31;4(1):18–9.
37. Mansur R, Gusmanizar N, Dahalan FA, Masdor NA, Ahmad SA, Shukor MS, et al. Isolation and characterization of a molybdenum-reducing and amide-degrading *Burkholderia cepacia* strain neni-11 in soils from west Sumatera, Indonesia. *IIOAB.* 2016;7(1):28–40.
38. Tornuk F, Ozturk I, Sagdic O, Yilmaz A, Erkmen O. Application of predictive inactivation models to evaluate survival of *Staphylococcus aureus* in fresh-cut apples treated with different plant hydrosols. *Int J Food Prop.* 2014;17(3):587–98.
39. Espeche MC, Tomás MSJ, Wiese B, Bru E, Nader-Macías MEF. Physicochemical factors differentially affect the biomass and bacteriocin production by bovine *Enterococcus mundtii* CRL1656. *J Dairy Sci.* 2014;97(2):789–97.
40. Li M, Niu H, Zhao G, Tian L, Huang X, Zhang J, et al. Analysis of mathematical models of *Pseudomonas spp.* growth in pallet-package pork stored at different temperatures. *Meat Sci.* 2013 Apr 1;93(4):855–64.
41. Tang X, Jin M, Sun W, Xie J, Pan Y, Zhao Y. Comparison of growth parameters of pathogenic and nonpathogenic *Vibrio parahaemolyticus* on cooked shrimp. *J Pure Appl Microbiol.* 2013;7(SPL.ISSUE):47–51.
42. Sevinç P, Gündüz U, Eroglu I, Yücel M. Kinetic analysis of photosynthetic growth, hydrogen production and dual substrate utilization by *Rhodobacter capsulatus*. *Int J Hydrog Energy.* 2012;37(21):16430–6.
43. Motulsky HJ, Ransnas LA. Fitting curves to data using nonlinear regression: a practical and nonmathematical review. *FASEB J Off Publ Fed Am Soc Exp Biol.* 1987;1(5):365–74.
44. Banerjee A, Ghoshal AK. Isolation and characterization of hyper phenol tolerant *Bacillus* sp. from oil refinery and exploration sites. *J Hazard Mater.* 2010;176(1–3):85–91.
45. Halmi MIE, Shukor MS, Johari WLW, Shukor MY. Mathematical modeling of the growth kinetics of *Bacillus* sp. on tannery effluent containing chromate. *J Environ Bioremediation Toxicol.* 2014;2(1):6–10.
46. Halmi MIE, Shukor MS, Johari WLW, Shukor MY. Evaluation of several mathematical models for fitting the growth of the algae *Dunaliella tertiolecta*. *Asian J Plant Biol.* 2014;2(1):1–6.
47. Halmi MIE, Ahmad SA, Syed MA, Shamaan NA, Shukor MY. Mathematical modelling of the molybdenum reduction kinetics in *Bacillus pumilus* strain Lbna. *Bull Environ Sci Manag.* 2014;2(1):24–9.
48. Skouloubris S, Labigne A, De Reuse H. Identification and characterization of an aliphatic amidase in *Helicobacter pylori*. *Mol Microbiol.* 1997 Sep;25(5):989–98.
49. Haldane JBS. *Enzymes*. Longmans, Green and Co. London; 1930.
50. Han K, Levenspiel O. Extended Monod kinetics for substrate, product, and cell inhibition. *Biotechnol Bioeng.* 1988;32(4):430–7.
51. Teissier G. Growth of bacterial populations and the available substrate concentration. *Rev Sci Instrum.* 1942;3208:209–14.
52. Aiba S, Shoda M, Nagatani M. Kinetics of product inhibition in alcohol fermentation. *Biotechnol Bioeng.* 1968 Nov 1;10(6):845–64.
53. Yano T, Koga S. Dynamic behavior of the chemostat subject to substrate inhibition. *Biotechnol Bioeng.* 1969 Mar 1;11(2):139–53.
54. Mulchandani A, Luong JHT, Groom C. Substrate inhibition kinetics for microbial growth and synthesis of poly- β -hydroxybutyric acid by *Alcaligenes eutrophus* ATCC 17697. *Appl Microbiol Biotechnol.* 1989;30(1):11–7.
55. Halmi MIE, Shukor MS, Masdor NA, Shamaan NA, Shukor MY. Testing the normality of residuals on regression model for the growth of *Paracoccus* sp. SKG on acetonitrile. *J Environ Bioremediation Toxicol.* 2015;3(1):15–17.
56. Halmi MIE, Shukor MS, Johari W.L.W WLW, Shukor MY. Mathematical Modeling of the Growth Kinetics of *Bacillus* sp. on Tannery Effluent Containing Chromate. *J Environ Bioremediation Toxicol.* 2014;2(1):6–10.
57. Akaike H. Factor analysis and AIC. *Psychometrika.* 1987;52(3):317–32.
58. Basak B, Bhunia B, Dutta S, Chakraborty S, Dey A. Kinetics of phenol biodegradation at high concentration by a metabolically versatile isolated yeast *Candida tropicalis* PHB5. *Environ Sci Pollut Res.* 2014;21(2):1444–1454.
59. Christen P, Vega A, Casalot L, Simon G, Auria R. Kinetics of aerobic phenol biodegradation by the acidophilic and hyperthermophilic archaeon *Sulfolobus solfataricus* 98/2. *Biochem Eng J.* 2012;62:56–61.
60. Saravanan P, Pakshirajan K, Saha P. Growth kinetics of an indigenous mixed microbial consortium during phenol degradation in a batch reactor. *Bioresour Technol.* 2008;99(1):205–9.